Duck plague virus infection alter the microbiota composition and intestinal functional activity in Muscovy ducks

Jie Kong,[*,†,‡] Xiuhong Wu,[*,†,‡] Liqin Liao,[*,†,‡] Zi Xie,[*,†,‡] Keyu Feng,[*,†,‡,§] Feng Chen,[*,†,‡,§] Xinheng Zhang,[*,†,‡,§,#] and Qingmei Xie[*,†,‡,§,#,1]

[*]*Heyuan Branch, Guangdong Provincial Laboratory of Lingnan Modern Agricultural Science and technology, College of Animal Science and Veterinary Medicine, South China Agricultural University, Guangzhou 510642, PR China;* [†]*Guangdong Engineering Research Center for Vector Vaccine of Animal Virus, Guangzhou 510642, PR China;* [‡]*South China Collaborative Innovation Center for Poultry Disease Control and Product Safety, Guangzhou 510642, PR China;* [§]*Key Laboratory of Animal Health Aquaculture and Environmental Control, Guangdong, Guangzhou 510642, PR China; and* [#]*Guangdong Provincial Key Lab of AgroAnimal Genomics and Molecular Breeding, College of Animal Science, South China Agricultural University, Guangzhou 510642, PR China*

ABSTRACT Intestinal damage from the duck plague virus (**DPV**) infection affects intestinal inflammation factors expression and barrier dysfunction. Here we report findings from the pathogenicity of the intestinal tract, intestinal morphological, intestinal permeability, inflammatory cytokines, and tight junction gene expression in 72 two-wk-old Muscovy ducks exposed to DPV. The characterization of intestinal metabolites and their classification were examined using 16-sequencing technology. The primary outcomes of the study evaluated the correlation between intestinal microbiota characteristics and the degree of infected tissue. The secondary outcomes were to determine whether the biosignatures that defined the microbiota were positively or negatively correlated with viral infection. The tissue was infected accompanied a mild damage of liver and spleen, and severe intestinal bleeding. Two inoculation routes were constructed with susceptible animals to assess the pathogenicity of the DPV in order to enrich the status of infection in Muscovy ducks. High levels of virus titer from Muscovy ducks were found being in the intestine. The expression of INF-α and IL-β with viral infection increased at 4, and 6 dpi, respectively, after detecting of the inflammatory factor and barrier function genes. At 4 and 6 dpi, barrier function gene of ZO-1 and Occludin reduced. The severity of viral infection was significantly correlated with the characteristics of the intestinal microbiota. Ducks infected with the DPV had an increase in the phylum *Firmicutes*, a decrease in the phylum *Actinobacteriota*, and differential enrichment with the genus *Bacteroides, Tyzzerella, Enterococcus*, and *Escherchia-Shigella*, while the genus *Rothia, Streptococcus*, and *Ralstonia* were differentially enriched in the control group. The findings from the current study demonstrated that DPV infection leads to an imbalance of the intestinal microbiota and disruption of the microbial homeostasis in the intestinal tissue in ducks, which might be one of the mechanisms whereby DPV infection might be established in Muscovy ducks. Na^+/K^+-ATPase and Ca^{2+}/Mg^{2+}-ATPase activity monitoring also showed that viral infection reduced these activities. These findings imply that changes in intestinal microbiota, intestinal barrier gene expression, and inflammatory factor are related to viral infection. When taken as a whole, this work provides fresh perspectives on the characteristics of intestinal microbiota and the infection damage caused by the DPV.

Key words: duck plague virus, inflammatory factor, barrier function gene, intestinal microbiota, physiological indicator

2023 Poultry Science 102:102365
https://doi.org/10.1016/j.psj.2022.102365

INTRODUCTION

Herpesviruses can be transmitted by direct contact or indirectly in the natural environment, susceptible hosts were easily infected, with mass mortality. These viruses invade intestine tissue after replication, which serves as a breeding ground for bacteria, viruses, and other microorganisms collectively known as the microbiota. The intestinal microbiota is essential for the host immune function, tissue development, and general health.

Received August 5, 2022.
Accepted November 27, 2022.
[1]Corresponding author: qmx@scau.edu.cn

Studies have shown that herpesvirus infections, such as Pseudorabies virus, cyprinid herpesvirus 2, Marek's disease virus, and cytomegalovirus, among others, might alter the microbiological composition and the pathophysiology of regulating immunity (She et al., 2017; Zhang et al., 2019; Bavananthasivam et al., 2021; Sbihi et al., 2022). Numerous studies have demonstrated that virus replication made a connection between the clinical signs and the intestinal microbiota (Figueroa et al., 2020; Kim et al., 2020; Erttmann et al., 2022). It is unknown, however, whether certain herpesviruses affect the intestinal microbiota in vivo or whether various inoculation methods have an equal impact on the pathogenicity of related viruses.

Duck plague virus (**DPV**) is a waterfowl pathogenic virus of the herpesviridae family that causes tissue failure and bleeding in the waterfowl (Dhama et al., 2017; El-Tholoth et al., 2019). Following the initial discovery of DPV in the Netherlands, this infectious disease with a sudden onset was seen in duck farms all over the world (Hanson and Willis, 1976; Aasdev et al., 2021; Islam et al., 2021; Khan et al., 2021). Affected ducks displayed similar symptoms, including severe manifestations of systemic hemorrhage, intestinal lesions, liver, and spleen hemorrhage. The waterfowl industry is seriously at risk since DPV can spread to a variety of duck species, including the cherry, white, saffron, and golden ducks, among others. Early research showed that DPV initially reproduced in the mucosa of the digestive tract before spreading to internal tissue and causing hemorrhagic necrosis of the intestine (Islam and Khan, 1995).

Pathogen invasion can alter the intestinal environment, induce intestinal damage, and exacerbate symptoms caused by infection (Spadoni et al., 2015; Prendergast et al., 2017; Oliva et al., 2021). An essential indicator of preserving intestinal health is intestinal microbial homeostasis (Sommer et al., 2017; Saez et al., 2021). Previously, we established that ducks were infected by DPV whether it is injected intravenously or intramuscularly, and here we enriched body damage in Muscovy ducks. Mucosal immunity is an important component of the humoral immune response (Zmora et al., 2017), and DPV infection is linked to the development of intestine associated genes that produce defenses against a variety of pathogens. The active role of intestinal immune function may be thought of as a mechanism of defense against pathogen invasion. Little is known about the study of viral infection on the characteristics of the intestinal microbiota of Muscovy ducks. The 14-days-old ducks used in the current study were intramuscularly and hypodermically injected with the virus. Clinical signs, body weight changes, pathological damage, virus distribution, intestinal microbiota, barrier function gene, and ATPase were systematically analyzed. This research laid the foundation for more thorough investigation into the pathogenic mechanism, which could considerably advance our understanding to intestinal microbiota function in DPV infection.

MATERIALS AND METHODS

Cell, Viruses, and Animal

DPV (BankIt2607498 Seq1OP205480) was provided from Waterfowl Department Wens, Guangdong, China. Specific-pathogen-free (**SPF**) duck embryos were obtained from the Harbin Veterinary Research Institute, Chinese Academy of Agricultural Sciences. Duck embryonic fibroblast (**DEF**) were isolated and propagated in Dulbecco's modified Eagle's medium (**DMEM**) supplemented with 5% fetal bovine serum (**FBS**) (Dang et al., 2021). One-day-old Muscovy ducklings free of DPV-specific maternal antibody were obtained from the WENS, Guangdong, China.

Cell Infection and Viability

To observe viral growth characteristics in vitro, primary cell that is commonly used to isolate DPV was selected of DEF in this study (Mondal et al., 2010). DEF cells were infected with DPV at a multiplicity of infection (**MOI**) of 0.5 or 1, respectively, while control group was cultured in DMEM and incubated at 37°C for various time periods. After that, cells were maintained in 2% FBS DMEM after being rinsed 3 times with phosphate-buffered saline (**PBS**). Each well was added to 10 μL of the Cell Counting Kit-8 solution (**CCK-8**) (Hernandez et al., 2021). Cell was further incubated for 4 h. About 450 nm absorbance was measured using a microplate reader.

Indirect Immunofluorescence Assay

To perform the immunofluorescence assays, the DEF was cultured from preprepared in 6 well-plate was used. At 24 h, cells were challenged by DPV until 72-h-post inoculation (**hpi**). After drying, cells were rinsed and fixed with 4% paraformaldehyde at room temperature for 15 min (Shi et al., 2022). Cells were next subsequently incubated with positive serum against DPV for 1 h, after which they were incubation with 1:2,000 diluted rabbit antigoat IgG (**H+L**) secondary antibody, electron fluorescence microscopy was used to examine the preparations, and Adobe Photoshop was used to edit the obtained photos.

Animal Experimental Design

Seventy-two, 2-wk-old Muscovy ducks with negative sera against the DPV were randomly divided into 4 groups and kept in isolators with negative pressure, and unrestricted access to food and water after receiving ethics approval by the Research Ethics Committee and Institutional Animal Care and Use Committee of South China Agricultural University. Ducks of the

Table 1. Sequence of primers used in qRT-PCR to detect inflammatory factors and barrier function gene expression.

Primer	Forward sequence (5′−3′)	Reverse sequence (5′−3′)
ZO1	TTCGGGAAGCTGGGTTTCTC	CCAGCGTCTCTTGGTTCACT
Occludin	GTGAGTGTCCCAATGGTG	ATGGAACACCTATGGAACAC
IFN-α	CCGCAACCTTCACCTCAG	GGGCTGTAGGTGTGGTTC
IL-β	TCACAGTCCTTCGACATCTTCG	CCTCACTTTCTGGCTGGATGAG
GAPDH	ATGAGAAGTATGACAAGT	ATTATCTAGTGAGGTGAG

experimental groups were injected with the DPV by intramuscular injection (**i.m.** injections) or hypodermic injection (**i.h.** injections) at a dose of $10^{5.28}$ $TCID_{50}$ in a 200 μL volume, respectively, to examine clinical symptoms and gross lesions of Muscovy ducks in vivo (Lian et al., 2011). PBS was administered in equal dosages to the control group at the same inoculation location. Post inoculation, the ducks (n = 18 per each group) were put into separate negative pressure isolator. Every day, the health check and body status were evaluated. Euthanized animals in advance if they appeared mental depression. Three ducks from each group were euthanized. The remaining ducks at the end of the study were euthanized by the intravenous administration of sodium pentobarbital (100 mg/kg body weight).

Histology Examination, Genome Extraction, and Real-Time PCR Verification

For hematoxylin and eosin (**H&E**) staining, tissues from each group were infiltrated with paraformaldehyde at a 4% concentration (Zhou et al., 2020). A portion of the tissue was removed from the freezer at low temperature and homogenized in 2.0 mL of precooled PBS. A pair of particular primers (F:5′-GTATGATTGCGGATAGATA-3′, R:5′-CGACTGATAGGTATAGGT-3′, 78 bp) were used in PCR to detect viral DNA/RNA in tissue or blood, and were extracted using the SteadyPure Viral DNA/RNA Kit. To measure the viral titer in various tissues, the DPV genome was used as a template. The recycling product was then ligated with the pMD-19T vector to create a standard plasmid that served as a standard curve (Yu et al., 2013). Finally, tissue genome was extracted by SteadyPure Viral DNA/RNA Kit for real-time PCR. PCR reaction conditions were as follows: 95°C for 30 s, 34 cycles of amplification at 95°C for 10 s, and 60°C for 30 s, followed by a dissociation curve analysis step.

Assay of Intestinal Microbiota

The TIANamp Stool DNA Kit (TIANGEN, Beijing, China) was used to obtain intestinal bacterial genomic. The integrity of the DNA samples was examined using agarose gel electrophoresis after the DNA samples were quantified using a NanoDrop spectrophotometer (Thermo, Waltham, MA). Utilizing an Illumina NovaSeq platform, sequencing libraries were created using the NEBNext UltraTM IIDNA Library Prep Kit (Al Khatib et al., 2021). Species annotation was performed on the ASVs of each sample at various levels by classify-sklearn in QIIME2. After that, α-diversity and β-diversity were analyzed by QIIME2.

Barrier Function Gene Relative Expression

According to Trizol (Takara, Dalian, China) instructions, total RNA from intestinal tissues was isolated, and its reverse transcription resulted in cDNA (Wu et al., 2018). Real-time quantitative PCR (**RT-qPCR**) validation of gene levels using the specified gene primer. The primer sequences of genes for zonula occludens (**ZO**)-1, Occludin, interferon-α (**IFN-α**), interleukin-1β (**IL-1β**), and glyceraldehyde-3-phosphate dehydrogenase (**GAPDH**) are displayed in Table 1. The $2^{-\Delta\Delta}$CT approach was used to determine relative expression level of each gene (Rao et al., 2013). GAPDH was utilized as the reference gene in the ileum.

Estimation of ATPase Activity in the Intestine

A 5% sodium pentobarbitone intravenous injection was used to euthanize 6 ducks every time point, or 18 ducks per group (Yin et al., 2019). The 2−3 cm intestinal segments were flushed to collect intestinal mucosal tissue, which were then quickly frozen in liquid nitrogen. Using a 2 mL Eppendorf tube, appropriate frozen intestine segments were taken superficially. Each tube was then filled with either 250 μL of 1-mm-diameter sterile glass beads or 1 mL of 0.067 M phosphate buffer, pH 7.5. The tissues were homogenized in a low temperature homogenizer for 15 min at 3,500 rpm. A portion of tissue was kept at or below 80°C, while the remaining tissue underwent intestinal analyses using Na^+/K^+-ATPase and Ca^{2+}/Mg^{2+}-ATPase kits from Beijing BoxBio Science & Technology Co., Ltd. At 660 nm, the solution was read by a spectrophotometer (Nepal et al., 2021). The results were expressed in U/g of ATP.

Statistics

Data analysis was performed using SPSS 19.0 and GraphPad Prism 8.0. One-Way ANOVA was utilized in the analysis and comparisons. The results were expressed as mean ± standard deviation (**SD**). The statistics were considered significant at $P < 0.05$.

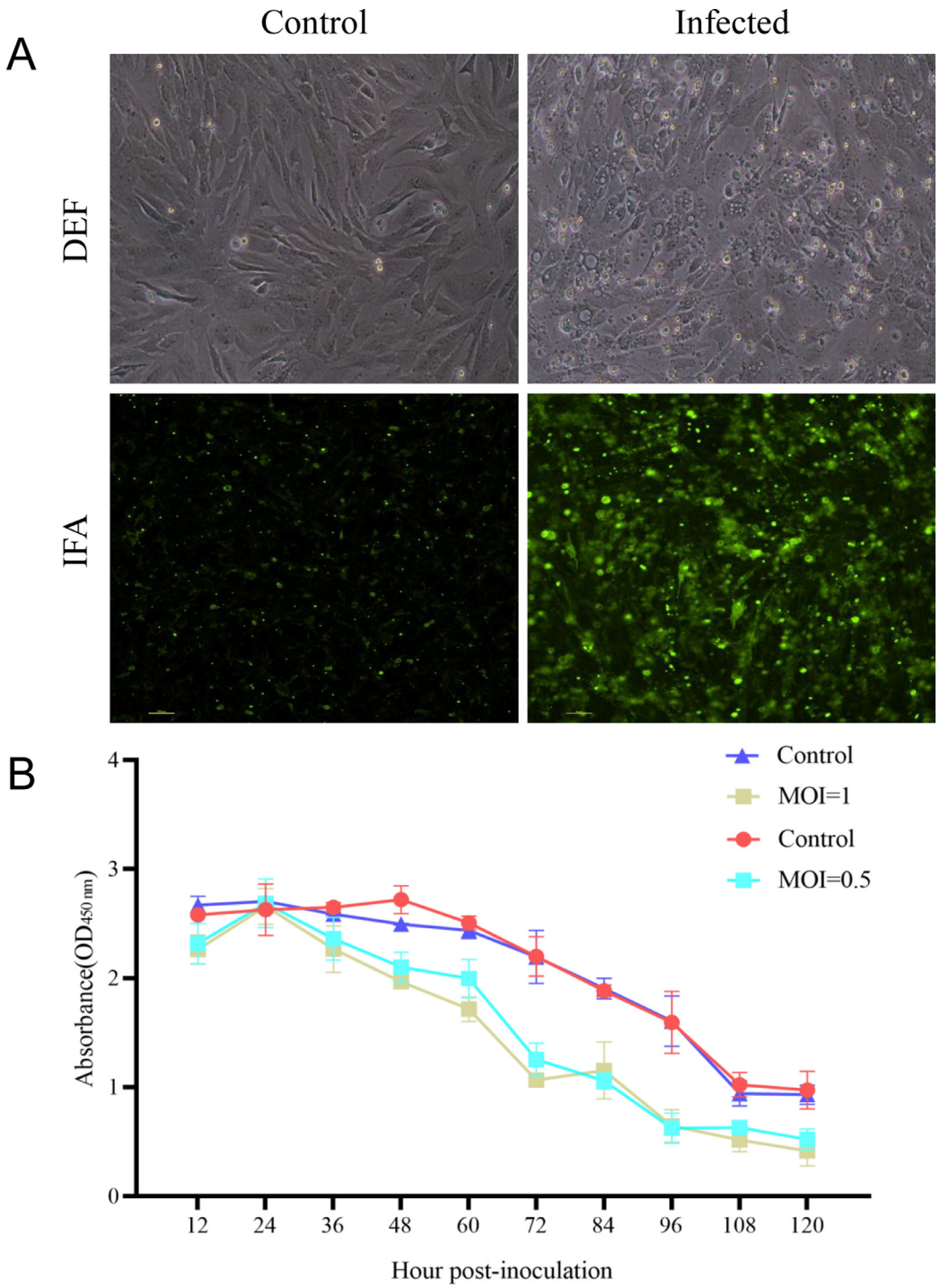

Figure 1. Replicative capacity of DEF cell infected with duck plague virus in vitro. (A) IFA analysis of DEF cells infected with duck plague virus during infection. (B) Effect of DEF cell viability during different infection time.

RESULTS

Identification and Cell Characterization of Infecting

DPV replicates efficiently in DEF cells. Normal duck primary cells appeared to exhibit a complete cell morphology in their microstructure. The endosomes were discovered in normal cell morphology at 3 to 4-day-post inoculation (**dpi**). Cells shed in vast quantities, up to death (Figure 1A). The immunological investigation was carried out by using positive serum of DPV, whereby immunofluorescence was observed to be fully emerged in the infected DEF cells (Figure 1B). DEF cells challenged by DPV at a MOI of 0.5 or 1 had decreased cell viability. Compared to the other groups, the infected group at a MOI of 1 had the lowest cell viability. Additionally, from 12 to 120 hpi, the infected group of cell viability was considerably decreased in comparison to the other groups (Figure 1C). These findings suggested that DEF cellular viability and survival could be adversely impacted by DPV infection.

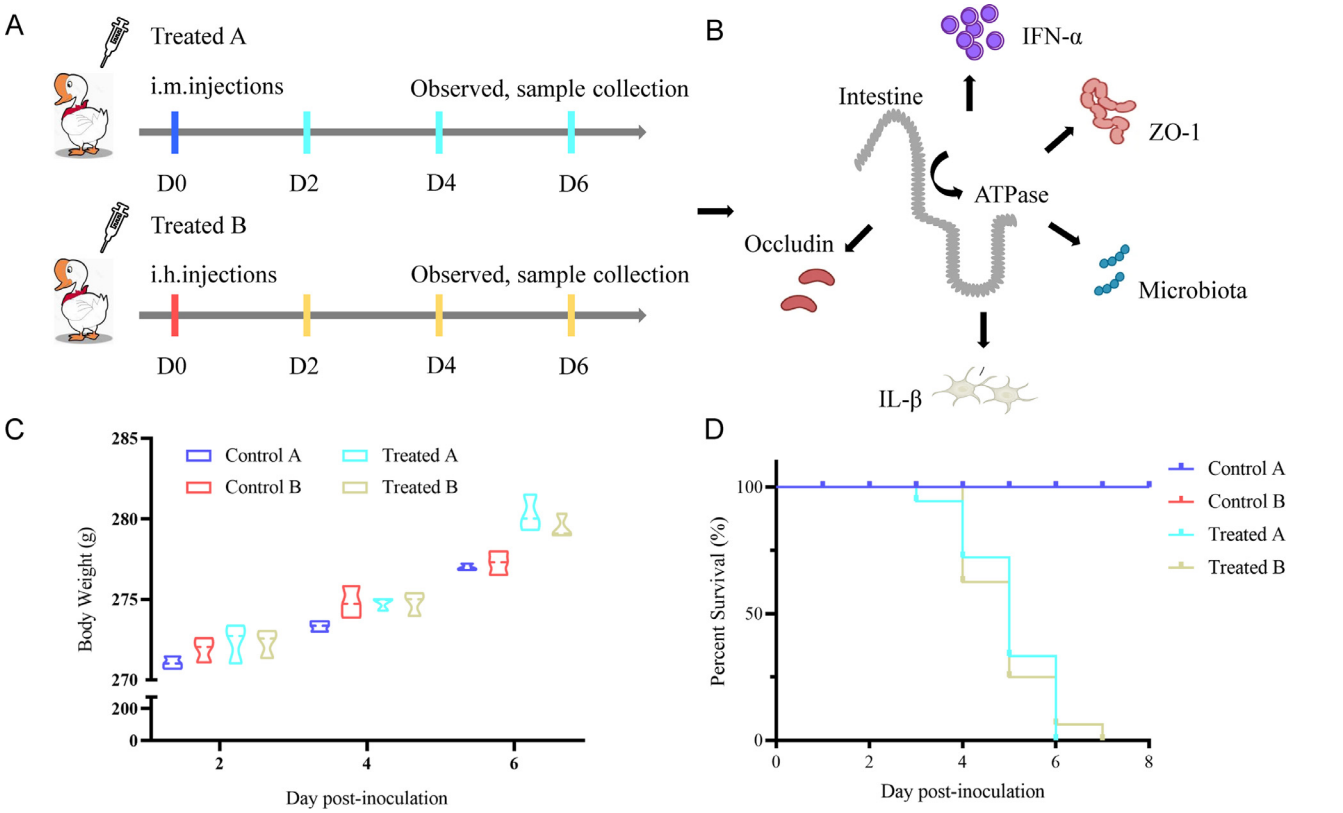

Figure 2. Diagram of animal regression experiments. (A) Muscovy ducks were randomly divided into 4 groups of 18. Two parallel control groups, and 2 experimental groups. Two-wk-old ducks of half of them were infected with corresponding DPV by i.m. injections or i.h. injections at a dose of $10^{5.00}$ $TCID_{50}$ in 0.1 mL volume. The half of the Muscovy ducks were used to as parallel negative controls. (B) Diagram is representative of several experiments related to intestinal infection. (C) The body weight of challenged Muscovy ducks. (D) The survival curves of challenged Muscovy ducks.

Clinical Observation and Weights Change in Ducks Infected With Duck Plague Virus

At the early infection stage (i.e., 2 dpi), none of the ducks in any group displayed clinical symptoms; however, at 3 dpi, a portion of the ducks began to exhibit listlessness, growth retardation, and decreased appetite in the i.m. injections group. The infected duck body weight began to grow at 4 dpi, and by 6 dpi it had clearly increased in comparison to normal ducks (Figure 2C). At 4 dpi, 4 ducks were found dead, and the rest infected ducks were found dead at 6 dpi. The majority of the ducks in the i.h. injection group displayed poor mental health by the third day, and at 4 and 5 dpi, over 60% of the ducks occur death. At 6 dpi, all the infected ducks died; no dead duck was observed in the corresponding control group (Figure 2D).

Pathological Injury of Tissue by Duck Plague Virus Infection

Liver, spleen, and intestine are key susceptible tissue of targets for DPV infection (Yuan et al., 2005; Shen et al., 2010). At the early infection stage (i.e., 2 dpi), none of the Muscovy ducks in any group displayed obvious injury; however, at 4 dpi, the liver surface of the infected groups was severely engorged (Figure 3A), the spleen was enlarged and engorged (Figure 3B), necrotic spots appeared in the intestine (Figure 3C), and some ducks only displayed other consistent symptoms like acute anorexia, diarrhea, sadness, and paralysis. At 6 dpi, postmortem examination of the infected ducks showed severe intestinal necrosis and congestion. There were large areas of necrosis and necrosis on the liver surface. The negative control ducks were euthanized and none of significantly histologic lesions were found.

The next phase involved determining whether the DPV intensifies tissue lesions in Muscovy ducks. As susceptible internal tissues, the liver, spleen, and intestine of the duck served as the first sources of sample collection. The control group did not develop any microscopic lesion throughout the experimental timeline. A high number of mildly enlarged hepatocytes and a sparse number of localized infiltrates of inflammatory cells were discovered in the livers that had been exposed to the infection for 2 dpi (Figure 3A). The white marrow of the spleen contained fewer cells, and there were several small areas of necrosis in the tissue (Figure 3B). In the intestine, epithelial cells were lost, but no other obvious abnormalities were present (Figure 3C). The remaining hepatocytes were closely arranged and more hepatic sinusoids and veins were stagnant at 4 dpi (Figure 3A). At this point, the white marrow structure was hazy, the area share was substantially reduced, and the red marrow, which contained a lot of red blood cells, showed

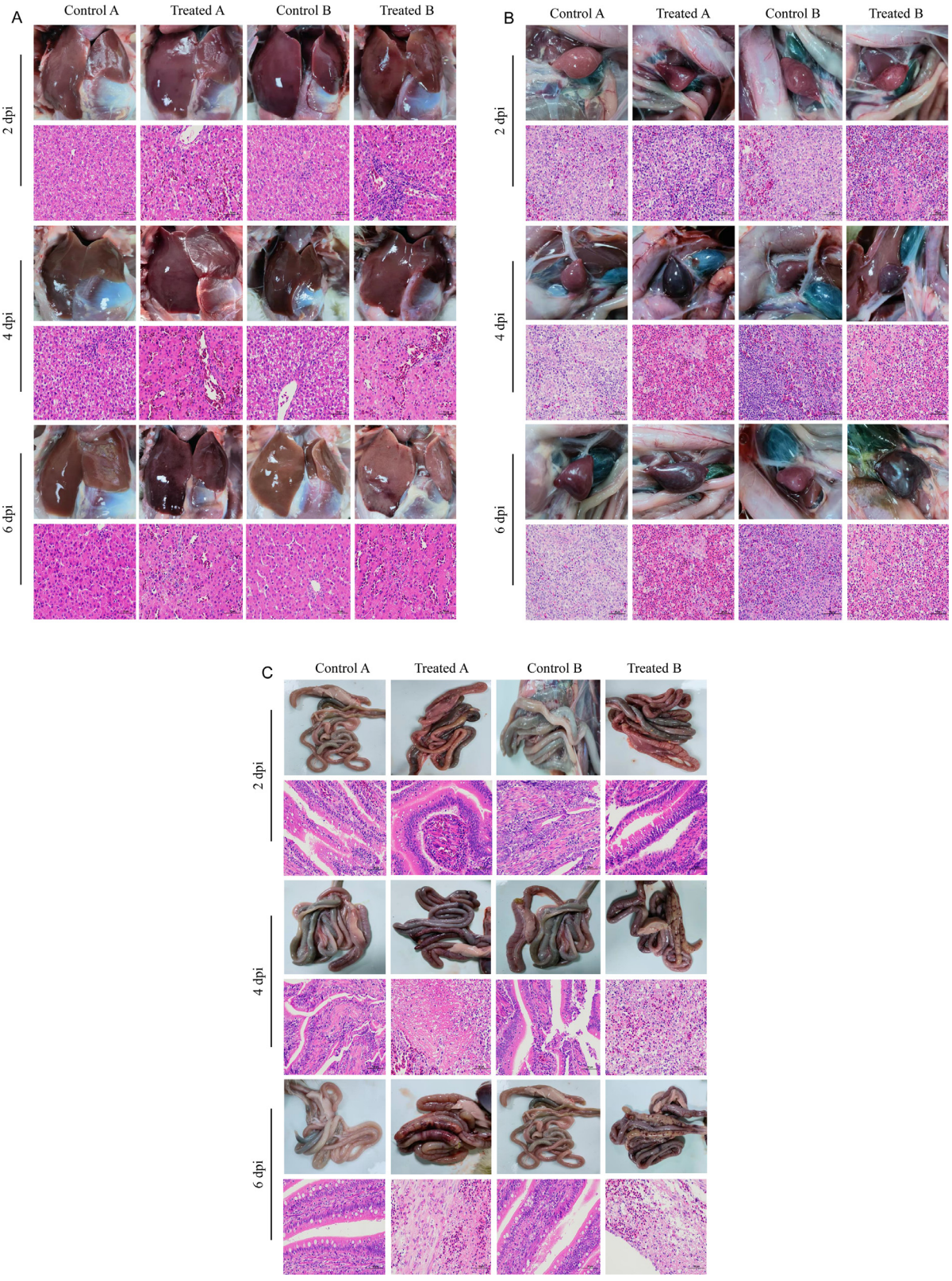

Figure 3. Infected capacity of DPV to Muscovy ducks in vivo. (A) Gross lesions and H&E-stained tissue of challenged ducks in livers. Enlarged livers with diffuse hemorrhage and necrosis; obvious fatty degeneration and basophilic inclusion bodies presented in hepatocytes, tissue structural disorders. From top to bottom are 2 dpi, 4 dpi, and 6 dpi. (B) Gross lesions and H&E-stained tissue of challenged ducks in spleens. Swelling, darkened, and spotted bleeding in spleen; various degrees of hemorrhage. From top to bottom are 2 dpi, 4 dpi, and 6 dpi. (C) Gross lesions and H&E-stained tissue of challenged ducks in intestine. Diffuse hemorrhagic spots on the intestinal surface, intestinal necrosis; massive villi breakage, and shedding. From top to bottom are 2 dpi, 4 dpi, and 6 dpi.

widespread bruising and hemorrhage (Figure 3B). A significant amount of inflammatory cell exudation, capillary bruising, and dilatation were also present, along with an enormous amount of necrotic tissue debris in the intestinal lumen. All challenged groups had more severe intestinal pathological damage at 6 dpi, with numerous

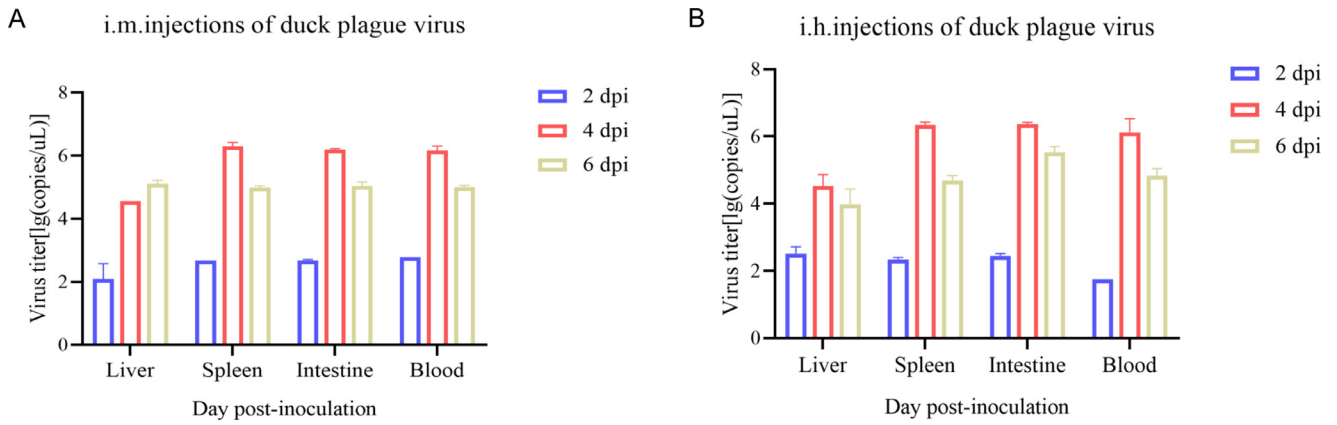

Figure 4. Growth kinetics of DPV in Muscovy ducks in vivo. (A) DPV effectively replicates in different tissue of the challenged ducks (i.m. injection group). (B) DPV effectively replicates in different tissue of the challenged ducks (i.h. injection group). Data are representative of different tissues related to viral infection. Virus titer were expressed as lg (copies/μL).

intestinal tissue necrosis, basic loss of the mucosal layer epithelium and intestinal glands, leaving only the exposed lamina propria connective tissue visible (Figure 3C).

Infectivity of Duck Plague Virus in Muscovy Ducks

To detect the DPV replication in Muscovy ducks, susceptible tissues of liver, spleen, and intestines were used as detection object. At 4 dpi, the spleen and intestine tissues had the highest viral titers. In the i.m. injection group, viral titers were 6.30 lg(copies/uL) and 6.19 lg (copies/uL) in the spleen and intestines, respectively (Figure 4A). In the i.h. injection group, Viral titers were 6.34 lg(copies/uL) and 6.38 lg(copies/uL) in spleen and intestines, respectively (Figure 4B). At 6 dpi, the viral titles of tissues started to decline, however intestinal tissue still had significantly high viral titers. The data demonstrated that DPV could efficiently replicate in Muscovy ducks, and that the virus reached its maximum titles in susceptible tissue at 4 dpi.

Viral Infection Affects the Diversity of Ileac Microbiota

We previously demonstrated DPV replication in the intestinal organoids, and the animal intestine can be used as the main research object for the modifications of microbiota by virus infection, and we evaluated the kinetics of viral replication. Within 4 dpi, a noticeably elevated viral load was seen in intestinal tissue. In total, we generated 961,146 raw reads sequences from 12 samples with an average read length of 411 bp. We acquired 744,074 optimized sequences, which were utilized to profile the intestinal microbiomes ASVs as proxies for bacterial species, after removing the primers, low-quality sequences, and filtering chimeras. Analysis of the rarefaction and rank abundance curves revealed that these curves tended to flatten as the number of sample sequences increased, indicating that the sample's richness and uniformity were sufficient, and that the sequencing depth was satisfactory (Figures 5A). These findings suggested that the sample quantity and level of sequencing were adequate. Nonmetric multidimensional scaling (**NMDS**) analysis reflects the differences between and within groups through the distance between points. The samples with high community structure similarity tended to cluster. Four groups might be created from the parts of all the groups in this study: R1 (T1, T2, and T3 of Treat A), R2 (J1, J2, and J3 of Treat B), R3 (C1, C2, and C3 of Control A), and R4 (C4, C5, and C6 of Control B). In the NMDS plot, a single area was shared by the points from the 2 treatment groups (R1 and R2) (Figure 5B).

Intestinal microbiota complexity was assessed using alpha-diversity indexes (Li et al., 2022). The greater Shannon and Chao1 indices indicate a more varied and diverse microbial population (Fan et al., 2021; Jiang et al., 2021). The Chao1 was used to contain the species richness of community sampled. When compared to the control group, the Chao1 of the R3, and R4 groups was significantly higher (Figure 5C). The variety of species, the total number of categories, and their proportions in the sample were all reflected using the Shannon index. The bigger the Shannon index, the more uniform the distribution of species is, and the higher the species diversity. Both treatment groups' Shannon indices were lower than those of the control group (Figure 5D). Consequently, these results demonstrated that the species richness and diversity in the Muscovy duck intestines might decrease following the DPV infection.

Composition of Intestinal Microorganisms at Different Levels

Additionally, we found *Firmicutes, Proteobacteria, Actinobacteria*, and *Bacteroidetes* in almost all intestinal tissues (Figure 6A). While *Actinobacteria* levels declined during the DPV infection, overall relative abundances of *Firmicutes, Proteobacteria*, and *Bacteroidetes* increased. We discovered 7 dominant Genus, including *Escherichia-Shigella, Rothia, Ruminococcus torques, Streptococcus, Muribaculaceae, Bacterroides*, and *Tyzzerella* (Figure 6E). In comparison to R3, R4,

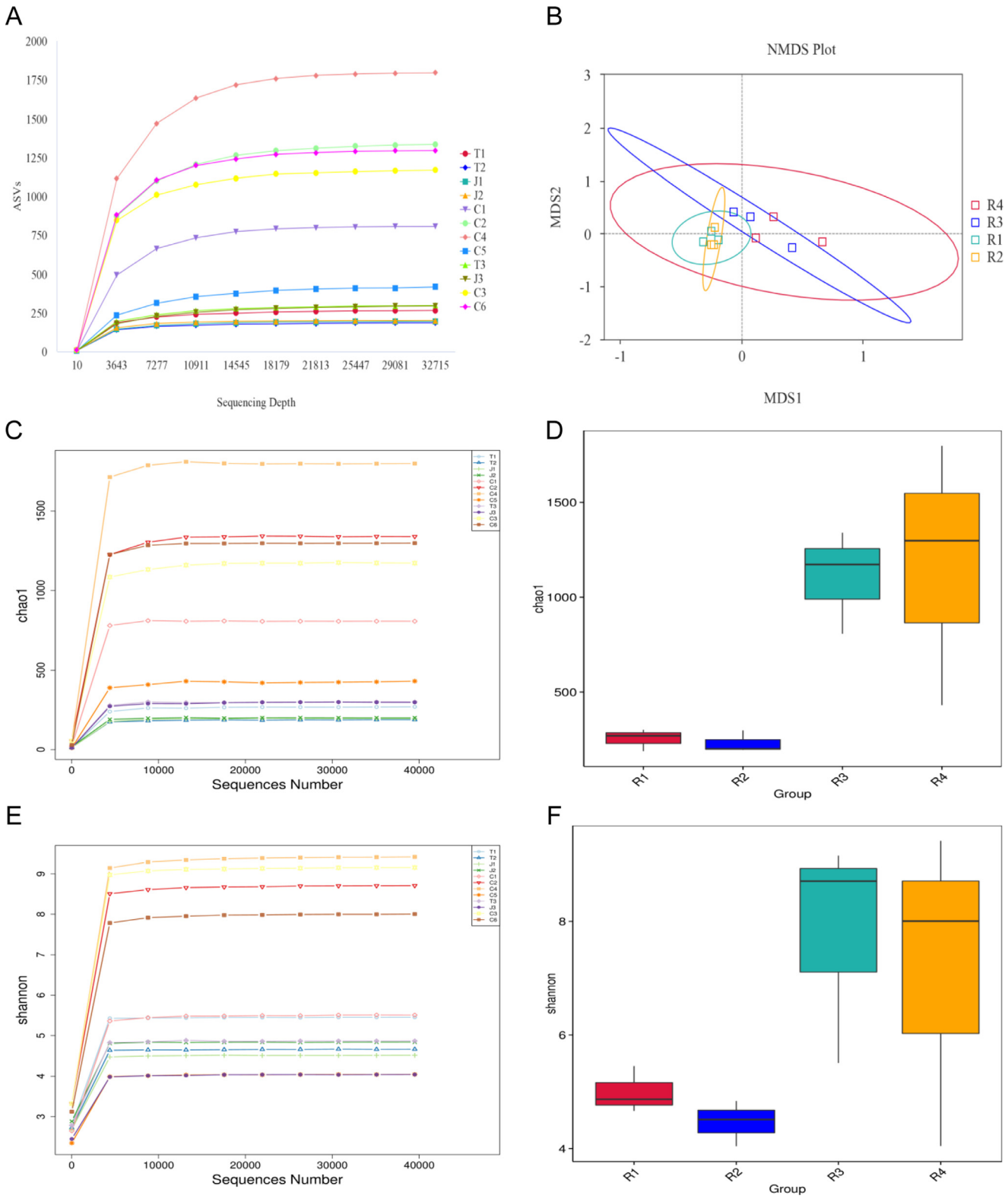

Figure 5. The diversity of intestinal microbiota in Muscovy ducks. (A) Rarefaction curve of experimental groups. The horizontal axis represents the amount of sequencing data, and the vertical axis represents the observed ASVs. (B) NMDS of microbial community structure in the treat groups and control groups. Symbols with different colors correspond to different groups. (C) The Chao 1 was used to estimate sample richness, and the horizontal axis represents the amount of sequencing data, and the vertical axis represents the corresponding alpha diversity index. (D) The horizontal axis represents grouping, while the vertical axis represents the corresponding alpha diversity index value. (E) Shannon indices were used to estimate sample diversity, and the horizontal axis represents the amount of sequencing data, and the vertical axis represents the corresponding alpha diversity index. (F) The horizontal axis represents grouping, while the vertical axis represents the corresponding alpha diversity index value.

Escherichia-Shigella, Ruminococcus torques, Bacteroides, and *Tyzzerella* in R1, R2 showed a substantial increase. In comparison to R3, R4, *Rothia, Streptococcus*, and *Muribaculaceae* in R1, R2 exhibited a considerable decline. The findings showed that intestinal tissues from treated groups and control groups exhibited distinct abundances, including 6 taxa at various levels (Figure 6).

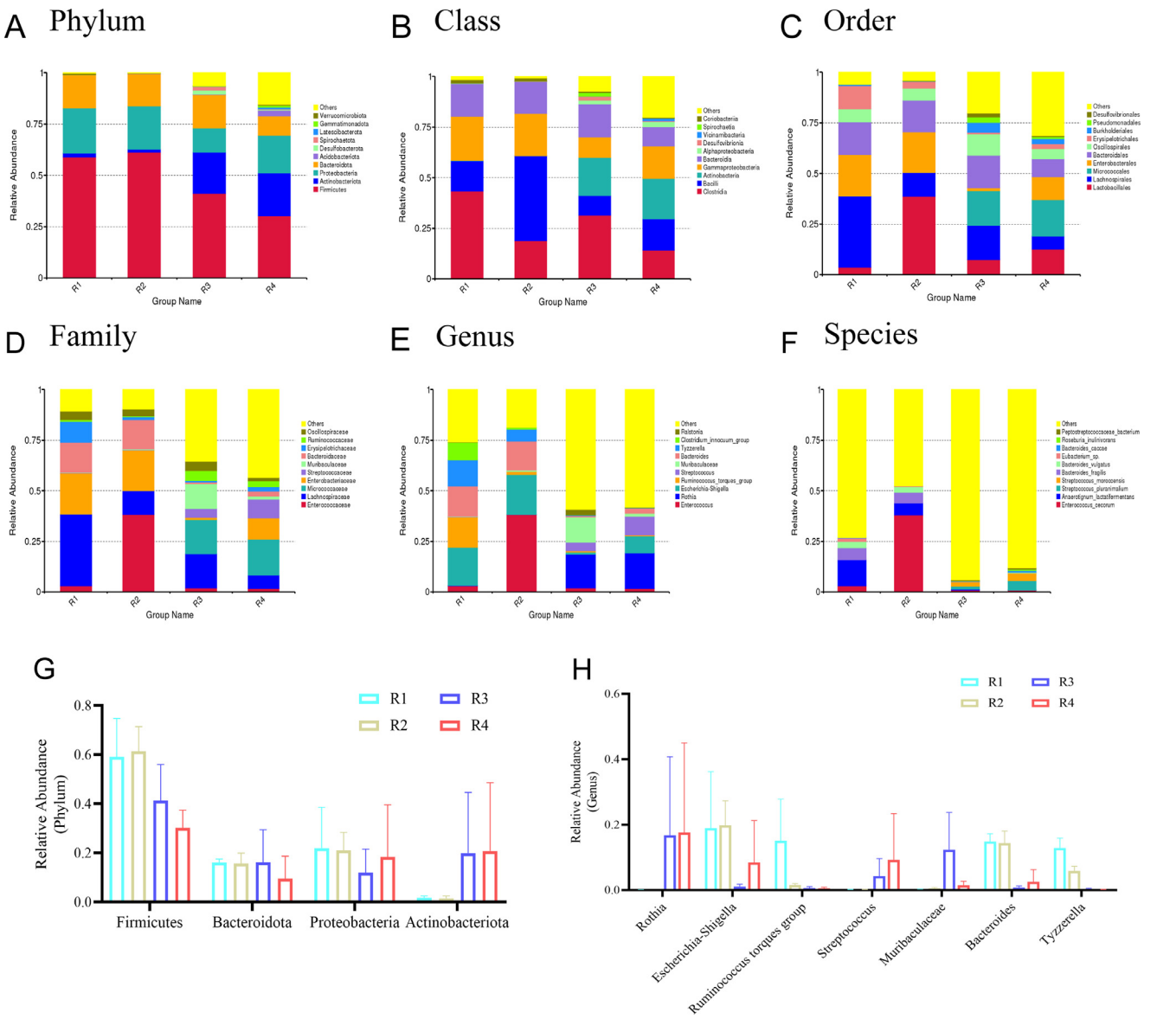

Figure 6. Relative abundance of intestinal microbiota in Muscovy ducks. (A) The bacterial community composition at Phylum level. (B) The bacterial community composition at Class level. (C) The bacterial community composition at Order level. (D) The bacterial community composition at Family level. (E) The bacterial community composition at Genus level. (F) The bacterial community composition at Species level. (G) Column chart represent the average relative abundance of the top 4 most abundant Phylum within intestine. (H) Column chart represent the average relative abundance of the top 7 most abundant Genus within intestine.

Gene Expression Associated With Intestinal Barrier Function and Inflammatory Factors

We then evaluated the associated gene expression of the DPV infection in the intestinal tissue between the infected treatment and the corresponding control groups using relative RT-qPCR. Viral infection may reduce the barrier function in the intestinal epithelium, preventing the intestinal mucosa from acting as its critical defensive barrier function. As shown in Figure 7, the expression levels of ZO-1 and Occludin gene were increased during after DPV infection (2–4 dpi) ($P < 0.05$), especially in the i.m. injections group. The expression levels of barrier function genes slightly decreased with the prolongation of time (4–6 dpi), indicating the DPV damages the intestinal barrier in the middle of infection (Figure 7C and D). We next assessed the inflammatory factors response of intestinal upon DPV infection. The results showed that compared with the control groups, the expressions of IFN-α and IL-β were all significantly up-regulated ($P < 0.01$), indicating that the infection of DPV would increase the expression of intestinal inflammatory cytokines. Notably, the expression level of inflammatory factors was highest in the late stage of DPV infection (6 dpi) (Figure 7A and B).

Na^+/K^+-ATPase, Ca^{2+}/Mg^{2+}-ATPase Inhibition in Intestinal After Viral Infection

Last but not least, we attempted treatment from the various groups of infection with DPV in vitro to look at whether intestinal infection with DPV might impact ATPase. The activities of Na^+/K^+-ATPase and Ca^2

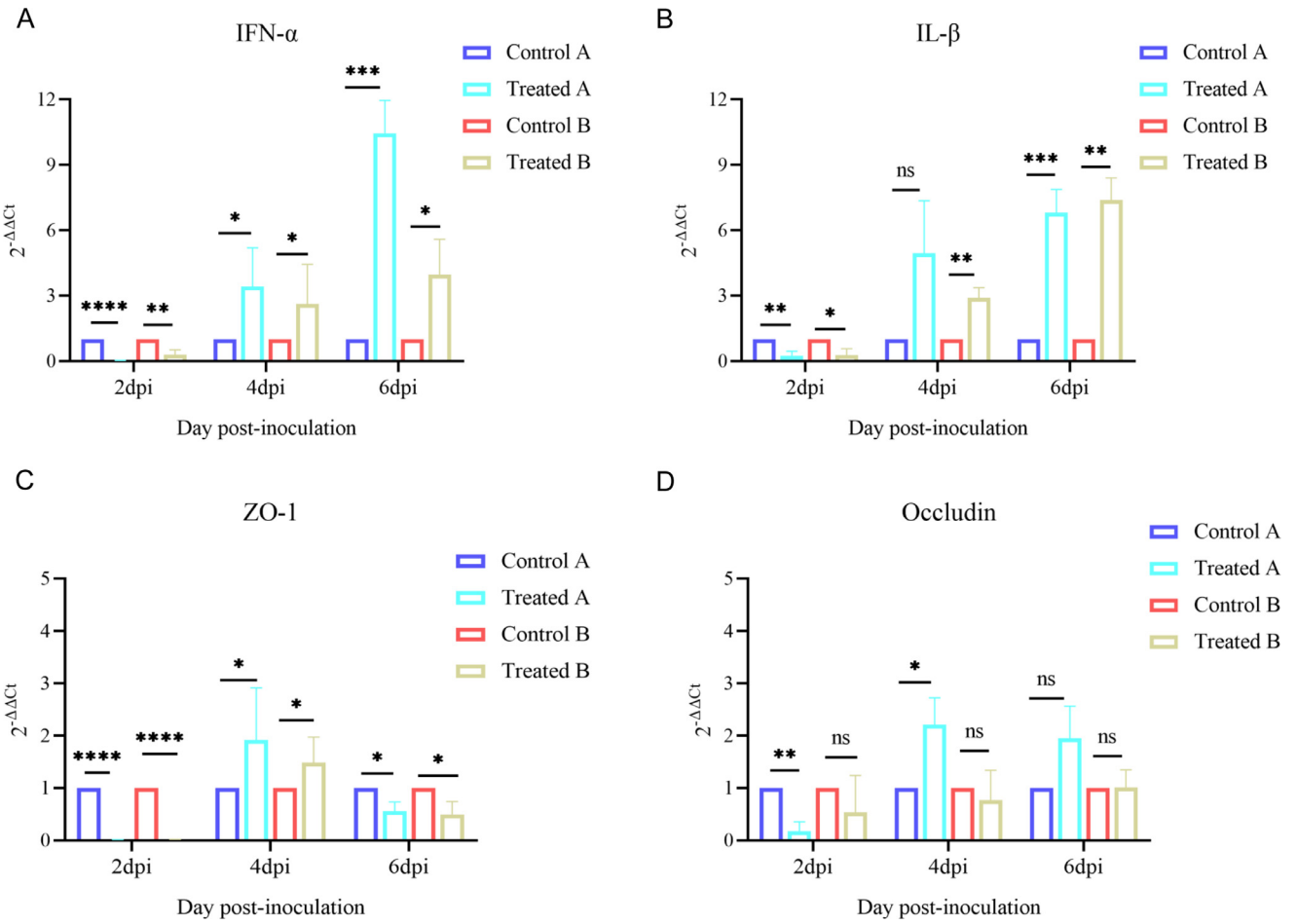

Figure 7. Gene expression of intestinal tissue in Muscovy ducks. Charts A to D show the expression of IFN-α, IL-β, ZO-1, and Occludin genes in intestinal tissues at 2 dpi, 4 dpi, and 6 dpi. mRNA levels were expressed as $2^{-\Delta\Delta CT}$.

$^{+}/Mg^{2+}$-ATPase were both impacted by virus replication in intestinal tissues, with suppression of ATPase being the most prominent effect. Interestingly, intestinal Na^{+}/K^{+}-ATPase and Ca^{2+}/Mg^{2+}-ATPase activity was negatively correlated with infection time. In this work, the activity of Na^{+}/K^{+}-ATPase and Ca^{2+}/Mg^{2+}-ATPase was examined at 2, 4, and 6 dpi. Compared to the control group, both ATPase activities were considerably decreased in the infection group (Figure 8). These finding showed that viral infection may result in an imbalance between water and electrolytes, which may ultimately lead to the watery diarrhea and dehydration typical after DPV infection.

DISCUSSION

DPV, a highly pathogenic and infectious pathogen in waterfowl, has been extensively studied during the past few decades (Hall and Simmons, 1972; Yin et al., 2017; Sarmah et al., 2020). The current findings showed that regardless of the inoculation routes, the typical symptoms were easily seen in the infected groups. Notably, we found that ducks in the hypodermic injection group were more affected than those of the intramuscularly injected group in terms of survival curves, body weight changes, clinical symptoms, and gross injuries. This finding may be connected to the fact that intramuscular injection routes were easy to absorb, which are reportedly more successful than hypodermic injection. This may be due to the fact that different injection routes allow for varying amounts of effective virus to infect target cells. However, in the hypodermic injection group, virus particles enter the peripheral blood directly and reach all tissues through the blood circulation, resulting in tissue damage (Ruddy et al., 2019). This is in contrast to the intramuscular injection route, which is administered at a vascular rich site, and which has a highly effective dose of virus entering the target cells and can spread quickly through the blood in the body (Spruce et al., 2020; Yamada et al., 2021).

Different inoculation routes have been shown to cause intestinal tissue disruption in Muscovy ducks, and our results confirmed these findings by demonstrating severe intestine damage. In the early stages of infection (2 dpi), we found viral DNA in all tissues, suggesting that the virus may rapidly replicate and colonize in multiple internal tissue. Since the intestine contained the highest levels of DPV, this suggests that it may be the primary target tissue, it is compatible with the clinical anatomy as seen in the animal regression experiments.

By replicating and colonizing in internal tissue, DPV infection causes an acute, contact, septicemic infection. The pathogen is widely present in tissues, blood, oral and nasal secretions, and feces of sick ducks. The

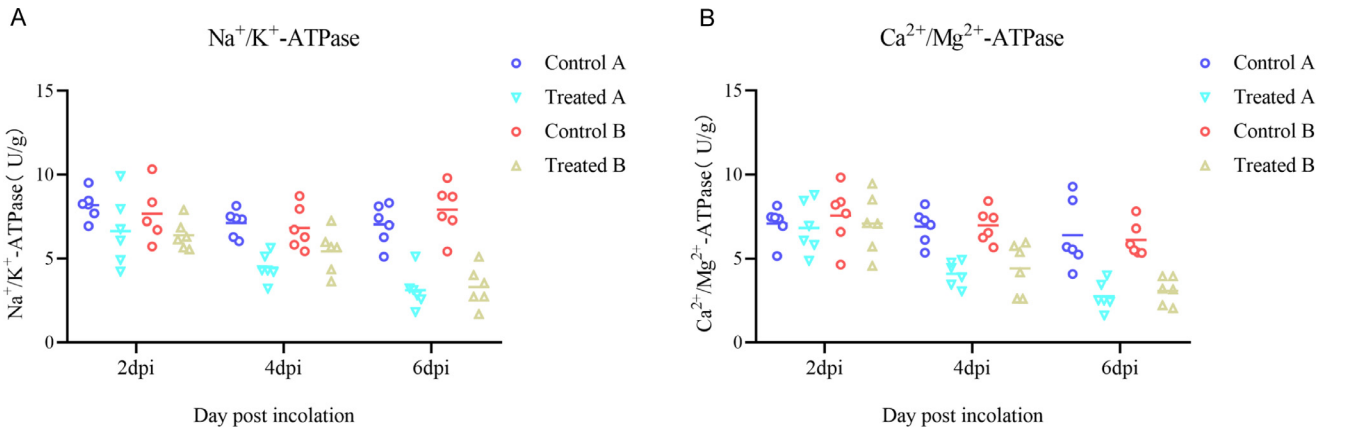

Figure 8. Effect of DPV infection on the ATPase activity in intestinal tissues. (A) Na^+/K^+-ATPase of 4 groups. (B) Ca^{2+}/Mg^{2+}-ATPase of 4 groups. Measurement of ATPase activity by commercial kits. Results are representative of 2 contents.

intestinal mucosal surface of ducks, like that of all vertebrates, is inhabited to a variety of microbiota that are essential to both health and disease (Yitbarek et al., 2018). Therefore, the aim of this study was to focus on assessing the effect of DPV infection on the composition of the intestinal microbiota. Our findings enrich to these conclusions by showing that viral infection destroys the diversity of the microbial flora. Nevertheless, we found that the ducks challenged reestablished the intestinal microbiota after its disruption, as seen by a restoration of α-diversity indexes microbial communities. We noticed the Phylum of the *Firmicutes, Proteobacteria*, and *Bacteroidetes* after infection close to that of the maximum level. Meanwhile, other bacteria Phylum, such as *Actinobacteria* which predominate, returned to low level following infection. Under nonchallenged circumstances, the makeup of the intestinal microbiota was kept. In addition, we identified 7 dominating Genus, and correlation analysis conducted throughout periods of relative species abundance supported the negative correlations between intestinal infection and *Rothia, Streptococcus*, and *Muribaculaceae*.

DPV infection can occur through the mucosal pathway, which includes the upper respiratory system and gastrointestinal tissues. It has been demonstrated that host intestine and host intestinal mucosa with viral infections cause a selective upregulation of an inflammatory factor. Inflammatory cytokines IFN-α and IL-β are strongly related to autoimmunity to infection, it was produced by cells infected with virus (Luo et al., 2021). To assess the cellular immune response in host body, the current study used 2 inflammatory cytokines, which are now also used as a marker of inflammatory status, in order to determine the impact of the DPV on cellular immunity in Muscovy ducks (Wang et al., 2018; Jian et al., 2021). Intriguingly, both the intramuscular and hypodermic injection groups showed a significant increase in IFN-α and IL-β gene expression at 4 to 6 dpi, it was maintained for a longer period of time. We also discovered a negative correlation between the degree of damage to the intestinal barrier factors and the expression levels of the intestinal barrier factors ZO-1 and Occludin, which decreased with increasing day of infection.

ATPases are transmembrane carrier proteins of mammalian cell membranes for ion transport, and normally, a steady membrane potential is typically required to ensure normal cellular function (Qu et al., 2019; Wang et al., 2019). The transmembrane potential difference ($\Delta\phi$) of the cell membrane therefore acts as the major source of energy states that support virus internalization during viral infection. An ion gradient that is comparatively steady on both sides of the cell is necessary for the normal structure and function of tissue cells. A decrease in Na^+/K^+-ATPase activity will result in intracellular Na^+ overload and K^+ reduction because Na^+/K^+-ATPase, a protease found in the cell membrane, is fundamentally responsible for maintaining the equilibrium of Na^+/K^+ both within and outside the cell. In the current investigation, compared to the control group, the intestinal mucosa of ducks infected with the virus had relatively lower Na^+/K^+-ATPase activity. Its decreased activity suggests that the disruption of intracytoplasmic ion homeostasis after infection was caused by the uptake of cytosolic Ca^{2+} and Mg^{2+} and the reduction of transmembrane efflux. The findings of this investigation demonstrated that, in contrast to the parallel control group, ducks infected with DPV had considerably lower intestinal Ca^{2+}/Mg^{2+}-ATPase activity. In conclusion, one of the biological processes of virus infection of the duck intestine may be the modification of Na^+/K^+-ATPase and Ca^{2+}/Mg^{2+}-ATPase activity.

Overall, the damage to the microbiota and pathogenicity in Muscovy ducks intestinal tissue appear to be related to the DPV infection. Beyond this specific influence, this suggests the existence of potential connections between the characteristics of the intestine microbiota, virus, and the inflammatory response. This is of considerable interest because it could lead to results with pathogenesis that could infect target tissue and better prevent epidemics.

ACKNOWLEDGMENTS

The authors gratefully acknowledge the Animal Experiment Center of South China Agricultural University for the support provided with the animal experiments, and

Prof. Feng Chen friendly provided the isolated and purified DPV strain.

This study was supported by National Key R&D Program of China (2022YFD1801000), Guangdong Provincial Key R&D Program (2020B020222001, 2019B1515210034, 2019A1515012006), the Chief expert Project of modern Agricultural Industry Technology innovation alliance in Guangdong Province (2020KJ128, 2021KJ128), the Science and Technology Program of Guangdong province, China (2020B1212060060), the China Agriculture Research System of MOF and MARA (CARS-42-13) and Provincial Science and Technology Special Fund Project for Zhongshan City (major special project + Task list management mode) (2021sdr003).

Ethics Statement: All experiments were carried out in strict accordance with the recommendations of the Guide for the Care and Use of Laboratory Animals of the National Institutes of Health. The use of animals in this study was approved by the South China Agricultural University Committee of Animal Experiments (approval ID: SYXK2019-0136).

Author contributions: K.J. designed the project and finalized the manuscript. X.H. and L.Q. performed the data analysis. J.F., X.Z., and K.Y. performed the experiments. C.F. provided the experimental material. X.H. and H.X. conducted the validation.

DISCLOSURES

The authors declare that the research was conducted in the absence of any commercial or financial relationships that could be construed as a potential conflict of interest.

REFERENCES

Aasdev, A., S. D. Pawar, A. Mishra, C. K. Dubey, S. S. Patil, S. M. Gogoi, D. P. Bora, N. N. Barman, and A. A. Raut. 2021. First complete genome characterization of duck plague virus from India. Virus Dis. 32:789–796.

Al Khatib, H. A., S. Mathew, M. K. Smatti, N. O. Eltai, S. A. Pathan, A. A. Al Thani, P. V. Coyle, M. A. Al Maslamani, and H. M. Yassine. 2021. Profiling of intestinal microbiota in patients infected with respiratory influenza A and B viruses. Pathogens 10:761.

Bavananthasivam, J., J. Astill, A. Matsuyama-Kato, K. Taha-Abdelaziz, and B. Shojadoost. 2021. Gut microbiota is associated with protection against Marek's disease virus infection in chickens. Virol. 553:122–130.

Dang, T. M., T. V. Le, H. Q. Do, V. T. Nguyen, A. X. L. Holterman, L. T. T. Dang, N. C. L. Phan, P. V. Pham, S. N. Hoang, L. T. Le, G. Grassi, and N. H. Truong. 2021. Optimization of the isolation procedure and culturing conditions for hepatic stellate cells obtained from mouse. Biosci. Rep. 41:BSR20202514.

Dhama, K., N. Kumar, M. Saminathan, R. Tiwari, K. Karthik, M. A. Kumar, M. Palanivelu, M. Z. Shabbir, Y. S. Malik, and R. K. Singh. 2017. Duck virus enteritis (duck plague) - a comprehensive update. Vet. Q. 37:57–80.

El-Tholoth, M., M. F. Hamed, A. A. Matter, and K. I. Abou El-Azm. 2019. Molecular and pathological characterization of duck enteritis virus in Egypt. Transbound Emerg. Dis. 66:217–224.

Erttmann, S. F., P. Swacha, K. M. Aung, B. Brindefalk, H. Jiang, A. Hartlova, B. E. Uhlin, S. N. Wai, and N. O. Gekara. 2022. The gut microbiota prime systemic antiviral immunity via the cGAS-STING-IFN-I axis. Immunity 55 847-861 e810.

Fan, H. N., P. Zhu, J. Zhang, and J. S. Zhu. 2021. Mucosal microbiome dysbiosis associated with duodenum bulb inflammation. Microb. Pathog. 150:104711.

Figueroa, T., P. Bessiere, A. Coggon, K. M. Bouwman, R. van der Woude, M. Delverdier, M. H. Verheije, R. P. de Vries, and R. Volmer. 2020. The microbiota contributes to the control of highly pathogenic H5N9 influenza virus replication in ducks. J. Virol. 94:e00289–20.

Hall, S. A., and J. R. Simmons. 1972. Duck plague (duck virus enteritis) in Britain. Vet. Rec. 90:691.

Hanson, J. A., and N. G. Willis. 1976. An outbreak of duck virus enteritis (duck plague) in Alberta. J. Wildl. Dis. 12:258–262.

Hernandez, E. P., M. R. Talactac, R. J. S. Vitor, K. Yoshii, and T. Tanaka. 2021. An Ixodes scapularis glutathione S-transferase plays a role in cell survival and viability during Langat virus infection of a tick cell line. Acta Trop. 214:105763.

Islam, M. M., J. Islam, M. S. Islam, T. Ahamed, M. R. Islam, M. M. Khatun, and M. A. Islam. 2021. Duck virus enteritis (duck plague) outbreak in an Australian black swan (Cygnus atratus) flock at safari park in Bangladesh: a case report. J. Adv. Vet. Anim. Res. 8:557–562.

Islam, M. R., and M. A. Khan. 1995. An immunocytochemical study on the sequential tissue distribution of duck plague virus. Avian Pathol. 24:189–194.

Jian, Y., D. Zhang, M. Liu, Y. Wang, and Z. X. Xu. 2021. The impact of gut microbiota on radiation-induced enteritis. Front. Cell Infect. Microbiol. 11:586392.

Jiang, Z., J. Wang, Z. Shen, Z. Zhang, and S. Wang. 2021. Characterization of esophageal microbiota in patients with esophagitis and esophageal squamous cell carcinoma. Front. Cell Infect. Microbiol. 11:774330.

Khan, K. A., M. A. Islam, A. A. M. Sabuj, M. A. Bashar, M. S. Islam, M. G. Hossain, M. T. Hossain, and S. Saha. 2021. Molecular characterization of duck plague virus from selected Haor areas of Bangladesh. Open Vet. J. 11:42–51.

Kim, A. H., M. P. Hogarty, V. C. Harris, and M. T. Baldridge. 2020. The complex interactions between rotavirus and the gut microbiota. Front. Cell Infect. Microbiol. 10:586751.

Li, Z., J. Zhou, H. Liang, L. Ye, L. Lan, F. Lu, Q. Wang, T. Lei, X. Yang, P. Cui, and J. Huang. 2022. Differences in alpha diversity of gut microbiota in neurological diseases. Front. Neurosci. 16:879318.

Lian, B., A. Cheng, M. Wang, D. Zhu, Q. Luo, R. Jia, F. Liu, X. Han, and X. Chen. 2011. Induction of immune responses in ducks with a DNA vaccine encoding duck plague virus glycoprotein C. Virol. J. 8:214.

Luo, Q., X. Lei, J. Xu, A. Jahangir, J. He, C. Huang, W. Liu, A. Cheng, L. Tang, Y. Geng, and Z. Chen. 2021. An altered gut microbiota in duck-origin parvovirus infection on cherry valley ducklings is associated with mucosal barrier dysfunction. Poult. Sci. 100:101021.

Mondal, B., T. J. Rasool, H. Ram, and S. Mallanna. 2010. Propagation of vaccine strain of duck enteritis virus in a cell line of duck origin as an alternative production system to propagation in embryonated egg. Biologicals 38:401–406.

Nepal, N., S. Arthur, J. Haynes, B. Palaniappan, and U. Sundaram. 2021. Mechanism of Na-K-ATPase inhibition by PGE2 in intestinal epithelial cells. Cells 10:752.

Oliva, A., M. C. Miele, F. Di Timoteo, M. De Angelis, V. Mauro, R. Aronica, D. Al Ismail, G. Ceccarelli, C. Pinacchio, G. d'Ettorre, M. T. Mascellino, and C. M. Mastroianni. 2021. Persistent systemic microbial translocation and intestinal damage during coronavirus disease-19. Front. Immunol. 12:708149.

Prendergast, A. J., B. Chasekwa, S. Rukobo, M. Govha, K. Mutasa, R. Ntozini, and J. H. Humphrey. 2017. Intestinal damage and inflammatory biomarkers in human immunodeficiency virus (HIV)-exposed and HIV-infected Zimbabwean infants. J. Infect. Dis. 216:651–661.

Qu, F., S. Liu, C. He, J. Zhou, S. Zhang, Z. Ai, Y. Chen, Z. Yu, and D. Ni. 2019. Comparison of the effects of green and black tea extracts on Na(+) /K(+) -ATPase activity in intestine of type 1 and type 2 diabetic mice. Mol. Nutr. Food Res. 63:e1801039.

Rao, X., X. Huang, Z. Zhou, and X. Lin. 2013. An improvement of the 2^(-delta delta CT) method for quantitative real-time polymerase

chain reaction data analysis. Biostat. Bioinforma Biomath. 3:71–85.

Ruddy, B. P., C. Bullen, J. T. W. Chu, S. H. Jeong, B. Madadkhahsalmassi, J. W. McKeage, D. Svirskis, M. D. Tingle, J. Xu, and A. J. Taberner. 2019. Subcutaneous nicotine delivery via needle-free jet injection: a porcine model. J. Control Release 306:83–88.

Saez, A., R. Gomez-Bris, B. Herrero-Fernandez, C. Mingorance, C. Rius, and J. M. Gonzalez-Granado. 2021. Innate lymphoid cells in intestinal homeostasis and inflammatory bowel disease. Int. J. Mol. Sci. 22:7618.

Sarmah, H., M. Shah, M. Pathak, N. N. Barman, M. Koul, A. Gupta, P. J. Sahariah, S. Neher, S. K. Das, S. M. Gogoi, and S. Kumar. 2020. Pathodynamics of circulating strains of duck enteritis virus: a step forward to understand its pathogenesis. Avian Dis. 64:166–173.

Sbihi, H., K. E. Simmons, M. R. Sears, T. J. Moraes, A. B. Becker, P. J. Mandhane, P. Subbarao, D. L. Y. Dai, B. B. Finlay, S. E. Turvey, and S. Gantt. 2022. Early-life cytomegalovirus infection is associated with gut microbiota perturbations and increased risk of atopy. Pediatr. Allergy Immunol. 33:e13658.

She, R., T. T. Li, D. Luo, J. B. Li, L. Y. Yin, H. Li, Y. M. Liu, X. Z. Li, and Q. G. Yan. 2017. Changes in the intestinal microbiota of Gibel carp (Carassius gibelio) associated with Cyprinid herpesvirus 2 (CyHV-2) infection. Curr. Microbiol. 74:1130–1136.

Shen, F. X., G. P. Ma, A. C. Cheng, M. S. Wang, C. F. Li, K. F. Sun, H. Chang, D. K. Zhu, R. Y. Jia, X. Y. Chen, and T. Sun. 2010. Development and application of an indirect immunohistochemical method for the detection of duck plague virus vaccine antigens in paraffin sections and localization in the vaccinated duckling tissues. Poult. Sci. 89:1915–1923.

Shi, X., X. Zhang, H. Sun, C. Wei, Y. Liu, J. Luo, X. Wang, Z. Chen, and H. Chen. 2022. Isolation and pathogenic characterization of duck adenovirus 3 mutant circulating in China. Poult. Sci. 101:101564.

Sommer, F., J. M. Anderson, R. Bharti, J. Raes, and P. Rosenstiel. 2017. The resilience of the intestinal microbiota influences health and disease. Nat. Rev. Microbiol. 15:630–638.

Spadoni, I., E. Zagato, A. Bertocchi, R. Paolinelli, E. Hot, A. Di Sabatino, F. Caprioli, L. Bottiglieri, A. Oldani, G. Viale, G. Penna, E. Dejana, and M. Rescigno. 2015. A gut-vascular barrier controls the systemic dissemination of bacteria. Science 350:830–834.

Spruce, M. W., C. A. Beyer, C. M. Caples, E. S. DeSoucy, H. W. Kashtan, G. L. Hoareau, J. K. Grayson, and M. A. Johnson. 2020. Pharmacokinetics of tranexamic acid given as an intramuscular injection compared to intravenous infusion in a swine model of ongoing hemorrhage. Shock 53:754–760.

Wang, J., H. Ji, S. Wang, H. Liu, W. Zhang, D. Zhang, and Y. Wang. 2018. Probiotic lactobacillus plantarum promotes intestinal barrier function by strengthening the epithelium and modulating gut microbiota. Front. Microbiol. 9:1953.

Wang, X. Y., T. Q. Zhao, D. P. Xu, X. Zhang, C. J. Ji, and D. L. Zhang. 2019. The influence of porcine epidemic diarrhea virus on pig small intestine mucosal epithelial cell function. Arch. Virol. 164:83–90.

Wu, C., Z. Yang, C. Song, C. Liang, H. Li, W. Chen, W. Lin, and Q. Xie. 2018. Effects of dietary yeast nucleotides supplementation on intestinal barrier function, intestinal microbiota, and humoral immunity in specific pathogen-free chickens. Poult. Sci. 97:3837–3846.

Yamada, M., K. Masujin, K. I. Kameyama, R. Yamazoe, T. Kubo, K. Iwata, A. Tamura, H. Hibi, T. Shiratori, S. Koizumi, K. Ohashi, M. Ikezawa, T. Kokuho, and M. Yamakawa. 2021. Experimental infection of pigs with different doses of the African swine fever virus Armenia 07 strain by intramuscular injection and direct contact. J. Vet. Med. Sci. 82:1835–1845.

Yin, D., P. H. Selle, A. F. Moss, Y. Wang, X. Dong, Z. Xiao, Y. Guo, and J. Yuan. 2019. Influence of starch sources and dietary protein levels on intestinal functionality and intestinal mucosal amino acids catabolism in broiler chickens. J. Anim. Sci. Biotechnol. 10:26.

Yin, H. C., L. L. Zhao, S. Q. Li, Y. J. Niu, X. J. Jiang, L. J. Xu, T. F. Lu, L. X. Han, S. W. Liu, and H. Y. Chen. 2017. Autophagy activated by duck enteritis virus infection positively affects its replication. J. Gen. Virol. 98:486–495.

Yitbarek, A., J. S. Weese, T. N. Alkie, J. Parkinson, and S. Sharif. 2018. Influenza A virus subtype H9N2 infection disrupts the composition of intestinal microbiota of chickens. FEMS Microbiol. Ecol. 94:10.

Yu, C. X., Z. Y. Zhao, J. X. Lv, and L. Zhu. 2013. A dual molecular beacon approach for fast detection of Mycobacterium tuberculosis. Mol. Biol. Rep. 40:1883–1892.

Yuan, G. P., A. C. Cheng, M. S. Wang, F. Liu, X. Y. Han, Y. H. Liao, and C. Xu. 2005. Electron microscopic studies of the morphogenesis of duck enteritis virus. Avian Dis. 49:50–55.

Zhang, C., Y. Liu, S. Chen, Y. Qiao, Y. Zheng, M. Xu, Z. Wang, J. Hou, J. Wang, and H. Fan. 2019. Effects of intranasal Pseudorabies virus AH02LA infection on microbial community and immune status in the ileum and colon of piglets. Viruses 11:518.

Zhou, J., C. Li, X. Liu, M. C. Chiu, X. Zhao, D. Wang, Y. Wei, A. Lee, A. J. Zhang, H. Chu, J. P. Cai, C. C. Yip, I. H. Chan, K. K. Wong, O. T. Tsang, K. H. Chan, J. F. Chan, K. K. To, H. Chen, and K. Y. Yuen. 2020. Infection of bat and human intestinal organoids by SARS-CoV-2. Nat. Med. 26:1077–1083.

Zmora, N., M. Levy, M. Pevsner-Fishcer, and E. Elinav. 2017. Inflammasomes and intestinal inflammation. Mucosal Immunol. 10:865–883.